

Effect of Ion-Neutral Collisions on Sheath Potential Profile

IEPC-2013-346

*Presented at the 33rd International Electric Propulsion Conference,
The George Washington University • Washington, D.C. • USA
October 6 – 10, 2013*

Samuel Langendorf¹, Mitchell L. R. Walker²
Georgia Institute of Technology, Atlanta, GA 30332, USA

Laura Rose³, Michael Keidar⁴
George Washington University, Washington, DC 20052, USA

Lubos Brieda⁵
Particle in Cell Consulting LLC, Falls Church, VA 22046

Abstract: To investigate the effect of ion-neutral collisions on plasma sheaths over floating surfaces, experimental measurements of near-wall plasma potential profiles are conducted in a multidipole plasma device with neutral pressures of 1 and 5 mTorr-Ar. Sheath and presheath potential profiles are measured over a HP grade boron nitride sample using an emissive probe, employing the technique of inflection points extrapolated to zero emission. Measured sheath thicknesses range from 0.9 to 1.4 cm while experimental ion-neutral mean free paths range from 1.2 to 6.0 cm, allowing both presheath and sheath length scales to be resolved. The plasma device generates electron number densities 1.3×10^{-7} and $1.9 \times 10^{-8} \text{ cm}^{-3}$. The electron energy distribution function is bi-Maxwellian with distinct hot (3.4 – 8.4 eV) and cool (0.7 – 0.8 eV) electron populations as measured by a planar Langmuir probe. The total potential drop observed across the measured sheaths ranges from 6.5 to 9 V, and the sheath electric field magnitudes are 8.5 - 13 V/cm. Experimentally measured potential profiles display agreement with the theoretical results of a fluid asymptotic matching solution for the sheath and presheath potential profile.

¹ Graduate Research Assistant, School of Aerospace Engineering, sam.langendorf@gmail.com

² Associate Professor, School of Aerospace Engineering, mitchell.walker@ae.gatech.edu

³ Graduate Research Assistant, School of Engineering and Applied Science, lauraprose@gwmail.gwu.edu

⁴ Associate Professor, School of Engineering and Applied Science, keidar@gwu.edu

⁵ Particle-in-cell Consulting Inc, Washington DC, lubos.brieda@particleincell.com

I. Introduction

ONE of the areas of uncertainty in modeling of electric propulsion (EP) devices is the interaction between the thruster discharge plasma and the walls that are exposed to it, such as the discharge chamber wall of a Hall effect thruster (HET) or the grids of an ion engine¹. This interaction is dominated by the plasma sheath, a transition region that develops between any plasma in contact with a wall in order to control positive and negative charge flux to the wall and satisfy the wall bias potential boundary condition (for the case of a floating wall, to balance charge fluxes and maintain a steady floating potential.)

Plasma sheaths have been recognized since Langmuir's seminal research in the field and have been the subject of a large number of theoretical publications over the past century,^{2,3} however few experimental observations of sheath potential profiles have been obtained to validate this theoretical development.⁴ This is due in part to the small physical dimensions of plasma sheaths in typical laboratory plasmas, and also due to the difficulty in making measurements within the sheath without introducing perturbations on equivalent or greater length scales. A 2005 review by Hershkowitz⁴ highlighted the need to explore the problem of sheaths in multi-species plasmas, and substantial progress has been made in that direction since 2005^{5,6}. However, in order to design the wall interaction in future EP devices, further experimental investigation is needed into the single species plasma sheath regarding the complication introduced by non-negligible ion-neutral collisions and the floating wall boundary condition.

To the knowledge of the author, experimental measurements of full sheath potential profiles are only presently available in the data of Oksuz and Hershkowitz at neutral pressures up to 0.44 mTorr, with presheath measurements at pressures up to 1 mTorr.⁷ In EP devices, the ionization region and to a lesser degree the acceleration region have substantial amounts of neutral propellant present, e.g. up to 10 mTorr in Ref. 8, and therefore it is desirable to measure sheath potential profiles at these increased ion-neutral collision frequencies and compare the results to theoretical predictions. In addition, EP devices often employ floating wall boundary conditions, for example in the ceramic discharge channel of a HET, so it is desirable to investigate sheath potential profiles over floating surfaces (not available in the data of Ref. 7 which was performed with a biased wall.) Consequently, the current work presents experimental measurements of both the sheath and presheath potential profiles over a floating HP grade boron nitride wall material sample at neutral pressures of 1 and 5 mTorr and compares the results to a fluid model.¹¹

II. Background

A collisional plasma sheath presents a multiple length scale problem, in which the pertinent scales are the electron Debye length λ_D and the ion-neutral collision mean free path λ . For $\lambda_D < \lambda$, the near-wall region is characterized by the highest electric field and the invalidity of quasi-neutrality. This size of this near-wall region, hereafter referred to as the 'sheath region,' scales with λ_D . Outside the sheath region, electric field decreases in magnitude but persists over a length that scales with λ ; this region is hereafter referred to as the 'presheath.' For $\lambda_D < \lambda$, the presheath region extends much farther into the bulk plasma than the sheath region; in the analysis of Hall effect thrusters, it is recognized that presheath electric fields can permeate the entire discharge plasma as illustrated in Figure 1, depending on magnetic field topography.⁹

An analytical technique commonly used to address this type of problem (a transition between regions governed by differing length scales, often termed a singular perturbation problem) is to compute the asymptotic expansions of the two regions and find a transition model that satisfies both expansions to a given order, a technique that is often referred to as the method of matched asymptotic expansions.¹⁰ For the case of plasma sheaths with non-negligible ion-neutral collisionality, such an analysis has been conducted by Riemann using a fluid model.¹¹ A parametric solution is found for arbitrary values of the λ_D/λ ratio. The transition region is found to scale as $\lambda_D^{4/5} \lambda^{1/5}$. Many other investigators using fluid models¹²⁻¹⁴ also recommend a scaling of $\lambda_D^{4/5} \lambda^{1/5}$, but their models are not directly compared in this paper.

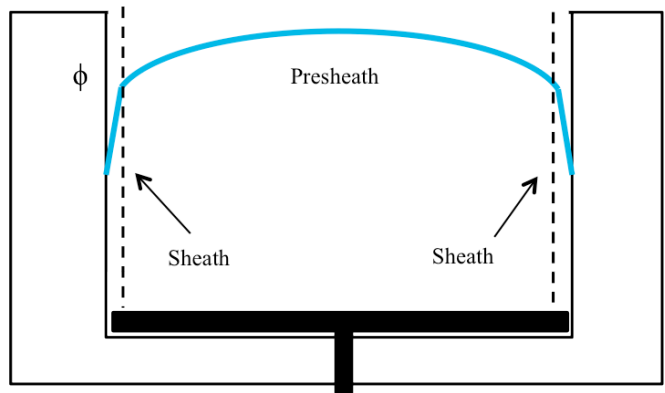


Figure 1. Schematic of sheaths and presheaths in a HET.

III. Experimental Method

To measure the potential profile in a sheath that contains ion-neutral collisions, a multidipole plasma device (so termed for its exterior array of permanent dipole magnets that provide primary electron confinement) is constructed in which electrons are generated thermionically from resistive heating of negatively biased tungsten filaments. A schematic of the plasma device is shown in Figure 2. The device is described in more detail in Ref. 15.

1. Neutral Pressure Environment

The multidipole plasma device is operated in the Georgia Institute of Technology Vacuum Test Facility 2, which is 9.2 meters long, 4.9 meters in diameter and uses ten CVI TM1200i cryopumps to achieve a base pressure of 1.9×10^{-9} Torr¹⁶. The plasma device is positioned in the center of the chamber. Six of the cryopumps are operated during this experiment. A 200 slm-N₂ range Dakota Instruments GC57 mass flow controller is used to flow 99.999% argon gas at a rate of $16 \pm 0.5 - 20 \pm 0.6$ slm-uncorrected radially into the chamber at a location 1.6 meters axial distance and 0.3 m radial distance from the plasma device center. Pressure is measured with $\pm 5\%$ accuracy using a MKS 626B 100 mTorr full scale capacitance manometer connected to the vacuum chamber using its 1-1/3" inch CF flange and a zero-length 2-3/4" to 1-1/3" CF adapter. The central positioning of the plasma device far from pumps and gas inlets should create a uniform neutral pressure throughout the plasma device and extending to the pressure measurement location due to molecular diffusion, so measured pressures are used to calculate experimental mean free paths without correction. A first-order 2D simulation of the neutral flow in the chamber supports this assertion, obtaining a pressure difference of 0.1 – 0.01 mTorr between the measurement location and the plasma device. The simulation uses a lattice Boltzmann BGK method and is implemented in COMSOL Multiphysics 4.3b.

The operating pressures selected yield ion-neutral mean free paths λ from 6 to 1.2 cm, assuming a constant collisional cross-section of 5×10^{15} cm⁻³ and calculating $\lambda = 1/\sigma_{in}n_n$, as verified theoretically in Ref. 17 and experimentally in Ref. 18. These mean free paths are substantially less than the characteristic length of the plasma device (~60 cm,) and are also significant fractions of the electron Debye lengths achieved (ratios $\lambda_D / \lambda = 0.030$ and 0.037 for the 1 mTorr and 5 mTorr cases, respectively.) Thus, the chosen cases are situations where both the presheath and sheath should be observable.

Argon is selected for these experiments rather than xenon, even though xenon is the most commonly used propellant for EP devices. This is to be able to compare operation with previous literature on multidipole devices (which generally used argon) and to achieve significant cost savings over xenon in light of the ~20 slm experimental flow rate. Using argon sacrifices little in terms of data utility, as the sheath theory investigated is easily varied between argon and xenon (a different value for ion mass) and there is little doubt that this aspect of the theory is justified and accurate.

2. Diagnostics

A planar Langmuir probe with a 0.56" diameter by 0.010" thick Tungsten collector is used to measure plasma parameters. The collector orientation is in plane with the central axis of the device. The probe holder is a 0.25" OD alumina tube. A cylindrical Langmuir probe is also included in the setup, however data collected from it is not used due to high variation in the probe characteristics as a function of sweep speed, indicating significant stray capacitance or a high contact resistance. A hairpin-type emissive probe is used to measure plasma potential, with 0.13 mm tungsten forming a 1.3 mm half-loop. The probe holder is a 1.5 mm OD double-bore alumina tube. The half-loop of the probe is oriented parallel to the wall surface to minimize 1D spatial in measurements. The probes are biased and the current read using a Keithley 2410 Sourcemeter, with signal carried by ~100 ft runs of RG-58A/U coaxial cable. Cable shields,

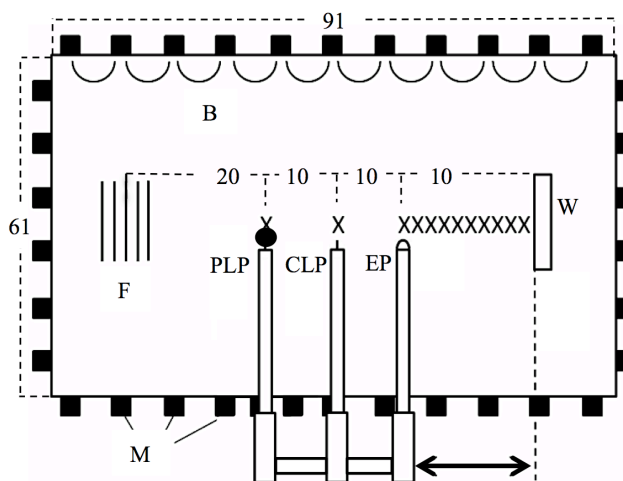


Figure 2. Schematic of experiment layout. *F* = filaments, *M* = magnets, *B* = nominal magnetic field, *PLP* = planar Langmuir probe, *CLP* = cylindrical Langmuir probe, *EP* = emissive probe, *W* = wall material sample, *X* = nominal data measurement location. Emissive probe orientation rotated 90° in figure to show hairpin tip geometry. Dimensions in cm, figure not to scale.

Sourcemeater chassis and chamber are connected to ground. The probes are positioned using a Parker 4062000XR linear motion table with a bi-directional repeatability of $\pm 5 \mu\text{m}$. The origin of the probe position is defined where the emissive probe support touches the wall, which is determined with accuracy of $\pm 125 \mu\text{m}$.

In the 1 mTorr case, the planar Langmuir probe is swept from -80 to +20 V in increments of 0.1 V, with a sweep period of 5 seconds. 25 sweeps are averaged to obtain a curve for data processing. In the 5 mTorr case, the probe is swept only 5 times but with increased integration dwell time specified in the Sourcemeater (0.1 power line cycles rather than 0.01.) The difference in sweeping speed is not expected to introduce large discrepancies between the measurements, as it is observed that I-V curves are similar between the two sweep speeds, with greater noise rejection at the higher dwell time. The bulk of the uncertainty in the interpretation of the diagnostics in this experiment comes from fluctuations in the mass flow rate, which are noted to correlate positively with the direction of drift in discharge current.

IV. Results and Discussion

Plasmas are generated at neutral pressures of 1 and 5 mTorr-Ar, with -60 V primary electron bias and 10.0 mA discharge current in both cases. Discharge current drifts were not recorded but generally stayed within 5% of nominal.

Figure 3 shows the results of the swept emissive probe measurements of sheath potential profile, with straight lines added to clarify the profile shape. Normalizing the profiles by their overall potential drop, it is observed that a greater portion of the overall potential fall takes place in the presheath as opposed to the sheath region. Figure 4 shows this outcome along with collisionless theory ($\lambda_D/\lambda \rightarrow 0$) fit to the near-wall sheath region.

Figure 5 shows the measured potential profiles compared with predicted profiles generated using the theory of Ref. 11, Langmuir probe data, and theory for the potential fall in the sheath over a floating wall. These foundations will be discussed prior to discussing the curves themselves.

	Prediction		Fit	
	5.0	1.0	5.0	1.0
p, mTorr	5.0	1.0	5.0	1.0
λ_D, mm	0.444	1.83	1.30	1.50
λ, mm	12.0	60.0	19.0	65.0
T_e, eV	0.73	1.07	0.70	0.8
$V_{\text{sheath}}, \text{V}$	-3.77	-5.54	-5.55	-8.38

Table 1. Input parameters to collisional sheath-presheath theory.¹¹ Constant collision frequency approximation used.

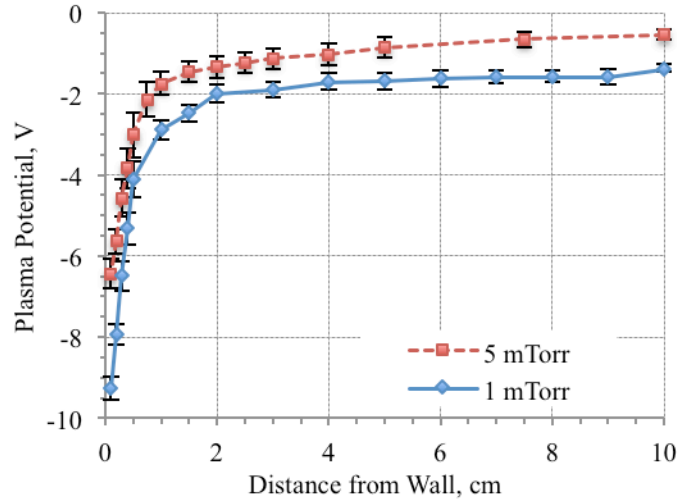


Figure 3. Measured sheath potential profiles.

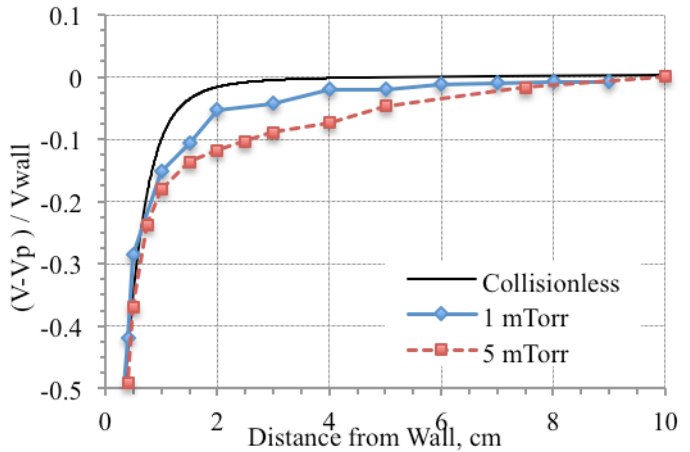


Figure 4. Measured sheath potential profiles normalized by wall potential. Collisionless theory added for comparison.

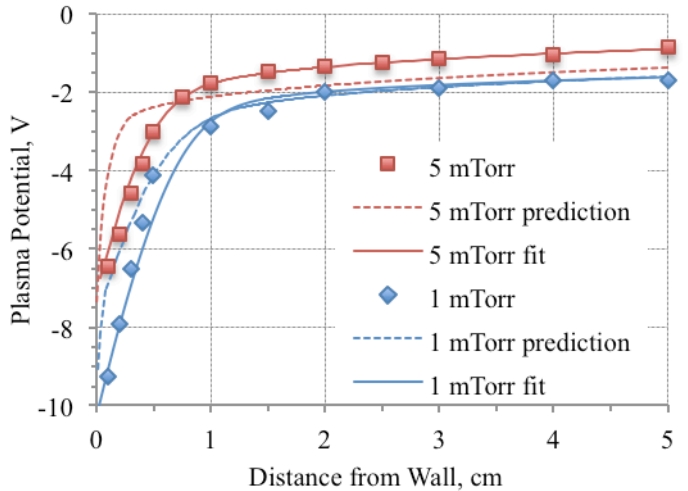


Figure 5. Measured potential profiles compared to fluid asymptotic matching theory.

A. Bi-Maxwellian Plasma

In order to dimensionalize a sheath model such as Ref. 11, values are required for Debye length (which scales the size of the sheath region,) the ion-neutral mean free path (which scales the size of the presheath region,) the plasma electron temperature (which scales the magnitude of the voltage,) and the voltage drop in the sheath region. All of these values can be estimated if measurements of the bulk plasma electron density and temperature are known, so the first step is to obtain these results from analysis of the Langmuir probe data.

Analysis of planar Langmuir probe measurements shows that the bulk plasma in this experiment exhibits a bi-Maxwellian electron energy distribution, which has been previously observed for multidipole plasma devices.^{Error! Bookmark not defined.} Analysis is performed using the first-derivative Druyvesteyn method described by Knapmiller et al. in Ref. 19. A linear fit to the square of the ion current is subtracted from the probe characteristics to isolate the electron current. The 1D electron energy distribution (normal to the probe surface) is calculated according to equation (5) in Ref. 19, reproduced below as equation (1).

$$f_1 = \frac{m}{q^2 A} \frac{dI_e}{d\phi} \quad (1)$$

The first derivative of electron current is calculated using a one-step finite difference, and the resulting plot of f_1 is shown in Figure 6. Also shown are the 1D Maxwellian distributions with n_e and T_e as free parameters which are fit to the data to minimize the sum of the square of the residual error between f_1 and the sum of the fitted distributions. Results are shown in Table 2, in which subscript 1 and 2 refer to the cooler and hotter electron populations respectively.

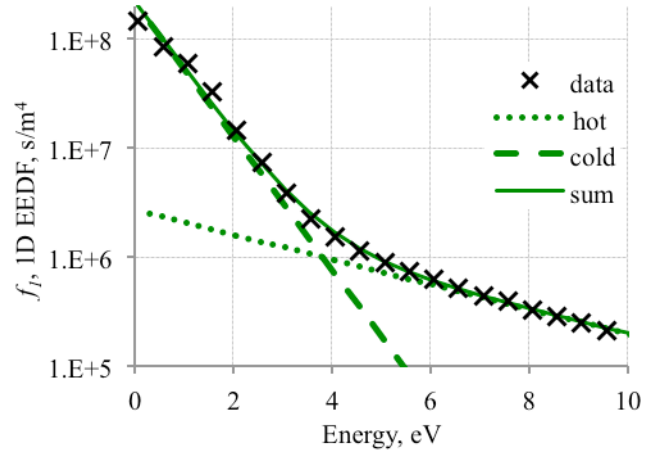


Figure 6. Planar Langmuir probe analysis. Measurements are performed using the first derivative of the electron current to obtain the 1D EEDF and least-squares fitted Maxwellians.

B. Floating Potential

Having obtained the electron temperatures and number densities, it remains to estimate the voltage drop in the sheath region to input to the theory of Ref. 11, which amounts to estimating the floating potential of the ceramic wall material sample. This input is necessary in order to provide a stopping condition for the numerical integration of the solution for the potential in the sheath region, which is when the potential has fallen the specified amount. This also sets the sheath thickness.

For a plasma with one electron temperature, the floating potential in an Argon plasma is calculated by equating ion (Bohm) and electron (Boltzmann) fluxes, resulting in equation (2) in which ϕ_f is the floating wall potential and μ is the ion / electron mass ratio:

$$\phi_f = -\frac{kT_e}{2e} \ln(0.43\mu) = -5.2 \frac{kT_e}{e} \quad (2)$$

Equation (2) relates floating potential to T_e , but for a bi-Maxwellian plasma with two electron temperatures it is not directly applicable unless an effective value can be chosen for T_e . Ref. 20 shows that the Bohm velocity in a bi-Maxwellian plasma is equivalent to that of a Maxwellian plasma with an electron temperature equal to the number density-weighted harmonic mean of the bi-Maxwellian electron temperatures, c.f. equation (3).

p	n_{e1}	n_{e2}	n_e	T_{e1}	T_{e2}	λ_D	λ
(mTorr-Ar)	(10^{13} m^{-3})	(10^{13} m^{-3})	(10^{13} m^{-3})	(eV)	(eV)	(cm)	(cm)
1 ± 0.15	0.95 ± 0.01	0.37 ± 0.04	1.3 ± 0.1	0.80 ± 0.1	8.4 ± 0.8	0.183 ± 0.04	6.0 ± 0.9
5 ± 0.35	18.9 ± 0.19	0.56 ± 0.06	19.4 ± 0.2	0.71 ± 0.1	3.8 ± 0.4	0.045 ± 0.01	1.2 ± 0.1

Table 2. Planar Langmuir probe measurements of bulk plasma parameters. First derivative theory and least-squares fitting of Maxwellian distributions is used to interpret I-V curves.

$$\frac{1}{T_e} = \left(\frac{n_{e1}}{n_e}\right) \frac{1}{T_{e1}} + \left(\frac{n_{e2}}{n_e}\right) \frac{1}{T_{e2}} \quad (3)$$

Alternatively, the floating potential of surfaces in a bi-Maxwellian plasma was derived by Godyak et. al²¹ in their treatment of the Tonks-Langmuir problem with a bi-Maxwellian plasma. Their result is equation (4) below, in which β is n_{e2}/n_e , δ is T_{e1}/T_{e2} , and $\eta_0 = 0.8539$.

$$\frac{\phi_f}{T_{e2}} = \frac{1}{\delta} \left\{ \frac{1}{2} \ln \left(\frac{\mu\pi\eta_0}{4} \right) + \ln \left(\frac{\beta}{\sqrt{\delta}} (1 + 0.292\beta) \right) \right\} \quad (4)$$

This result is qualitatively different than the harmonic mean result of equation (3), in that it is weighted toward the temperature of the hot electron population as opposed to the cold. Floating potentials predicted using equations (2-3) and equation (4) with the measured plasma parameters are -3.8 and -10.3 V respectively for the 5 mTorr case and are -5.5 and -45.3 V for the 1 mTorr case. The harmonic mean T_e method yields results in closer agreement with measurement and so these results are used to generate the ‘prediction’ profiles shown in Figure 5.

C. Theoretical Potential Profiles

Now, all the inputs to the implementation of the theory of Ref. 11 are available, and are summarized in Table 1. The resulting profiles and their relation to the experimental data are shown in Figure 5. All profiles are translated along the vertical (voltage) axis to roughly overlay – this is a degree of freedom in the model, reflecting the physical fact that bulk plasma potential may vary between systems. The prediction profiles have no other degree of freedom besides translation along the voltage axis; the position of the curve on the horizontal axis is fixed such that the potential drop in the sheath region is equal to the input value, which for the prediction profiles is calculated from the measured electron temperatures.

The prediction profiles are similar to the measured profiles, but display differences in slope / electric field strength, particularly in the sheath region. However it seems that the two-scale theory in general is a good representation of the sheath-presheath, as evinced by the ‘fit’ profiles. These profiles are generated by allowing the input parameters to vary to fit the measured data, until $R^2 > 0.98$. The fit profiles are picked by trial and error and quickly converged to $R^2 > 0.98$. The values that are used to generate the fit profiles are listed in Table 1. Because of the ready agreement of the fit and the apparent two-scale nature of the measured profiles, it is believed that the deviations observed in the prediction profiles is as likely the result of experimental error as of inappropriate theory. To compare the predictions in more detail, data must be obtained with increased spatial resolution, particularly in the transition region.

V. Conclusions

The potential measurements presented in this work provide an experimental validation of the fluid formalism of an asymptotically matched sheath-presheath potential profile, in which the sheath thickness is governed by λ_D and the presheath thickness by λ . This model should serve well for modeling of plasma-wall interactions in situations where collisional mean free paths are a relevant length scale to the degree expected in EP devices, with the qualification that other wall-interaction phenomena (SEE, magnetic fields) are not treated and should be incorporated if they are expected to be significant. The measured sheath potential profiles also provide results for the floating potential of an insulating wall, which do not agree with the results of bi-Maxwellian theory, however the method of a harmonic mean effective T_e agrees more closely. Further investigations are needed to decrease the range of experimental error and validate the measurements by comparing with the results of particle-in-cell simulation, however, these findings support the utility of the fluid asymptotic matching approach to the calculation of the sheath-presheath potential profile across the range of collisionality expected in electric propulsion devices.

Acknowledgments

This work is supported by the Air Force Office of Scientific Research through Grant FA9550-11-10160.

References

¹Shastry, R., "Experimental Characterization of the Near-Wall Region in Hall Thrusters and its Implications on Performance and Lifetime," Ph.D. Dissertation, University of Michigan, 2011.

²Langmuir, I., The interaction of electron and positive ion space charges in cathode sheaths. *Physical Review*, 33(6), 954, 1929.

-
- ³Allen, J. E. (2009). The plasma–sheath boundary: its history and Langmuir's definition of the sheath edge. *Plasma Sources Science and Technology*, 18(1), 014004.
- ⁴Hershkowitz, N., "Sheaths: More complicated than you think," *Physics of plasmas*, Vol. 12, p. 055502, 2005.
- ⁵Yip, C. S., Hershkowitz, N., and Severn, G., "Experimental test of instability-enhanced collisional friction for determining ion loss in two ion species plasmas," *Physical review letters*, Vol. 104, No. 22, p. 225003, 2010.
- ⁶Zhang, Z. and Wang, X., "Ion streaming instability in a plasma sheath with multiple ion species," *Plasma Physics and Controlled Fusion*, Vol. 54, No. 8, p. 082001, 2012.
- ⁷Oksuz, L. and Hershkowitz, N., "Plasma, presheath, collisional sheath and collisionless sheath potential profiles in weakly ionized, weakly collisional plasma," *Plasma Sources Science and Technology*, Vol. 14, No. 1, p. 201, 2005.
- ⁸Reid, B. M., "The Influence of Neutral Flow Rate in the Operation of Hall Thrusters," Ph.D. Dissertation, University of Michigan, 2009.
- ⁹Keidar, M., Boyd, I. D., & Beilis, I. I., "Plasma flow and plasma–wall transition in Hall thruster channel," *Physics of Plasmas*, 8, 5315, 2001.
- ¹⁰Van Dyke, M., *Perturbation Methods in Fluid Mechanics*, The Parabolic Press, Stanford, California, 1975.
- ¹¹Riemann, K. U., "The influence of collisions on the plasma sheath transition," *Physics of plasmas*, 4, 4158, 1997.
- ¹²Franklin, R. N., and Ockendon, J. R., "Asymptotic matching of plasma and sheath in an active low pressure discharge" 1970 *J. Plasma Phys.* 4.2 (1970): 371-385.
- ¹³Kaganovich, I. D., "How to patch active plasma and collisionless sheath: A practical guide." *Physics of Plasmas*, Vol. 9, 4788, 2002.
- ¹⁴Lam, S. H., Lam, S. H., Unified theory for the Langmuir probe in a collisionless plasma. *Physics of Fluids*, 8, 73, 1965.
- ¹⁵Langendorf, S., Walker, M. L. R., Rose, L. P., Keidar, M., Brieda, L., "Study of the Plasma-Wall Interface – Measurement and Simulation of Sheath Potential Profiles", *49th AIAA Joint Propulsion Conference*, San Jose, CA, 2013.
- ¹⁶Kieckhafer, A. W., Walker, M. L. R., "Recirculating Liquid Nitrogen System for Operation of Cryogenic Pumps," *32nd International Electric Propulsion Conference*, Hamburg, Germany, September 2011.
- ¹⁷Rapp, D., & Francis, W. E., "Charge exchange between gaseous ions and atoms," *The Journal of Chemical Physics*, Vol. 37, 2631, 1962.
- ¹⁸Kobayashi, N., "Low Energy Ion-Neutral Reactions. VI. $\text{Ar}^{++} \text{Ar}$, $\text{Nt}^+ \text{N}_2$, $\text{O}_2^{++} \text{O}_2$ and $\text{CO}^{++} \text{CO}$," *Journal of the Physical Society of Japan*, Vol. 38 (2), 1975.
- ¹⁹Knappmiller, S., Robertson, S., Sternovsky, Z., "Method to find the electron distribution function from cylindrical probe data," *Physical Review E*, 73(6), 066402, 2006.
- ²⁰Song, S. B., Chang, C. S., & Choi, D. I., "Effect of two-temperature electron distribution on the Bohm sheath criterion," *Physical Review E*, Vol. 55, No. 1, 1213, 1997.
- ²¹Godyak, V. A., Meytlis, V. P., Strauss, H. R., "Tonks-Langmuir Problem for a Bi-Maxwellian Plasma," *IEEE Transactions on Plasma Science*, Vol. 23, No. 4, 1995.